

## Non-equilibrium Kondo effect in asymmetrically coupled quantum dot

M. Krawiec and K. I. Wysokiński

Institute of Physics, M. Curie-Skłodowska University,  
ul. Radziszewskiego 10A, 20-031 Lublin, Poland

(dated: March 22, 2024)

The quantum dot asymmetrically coupled to the external leads has been analysed theoretically by means of the equation of motion (EOM) technique and the non-crossing approximation (NCA). The system has been described by the single impurity Anderson model. To calculate the conductance across the device the non-equilibrium Green's function technique has been used. The obtained results show the importance of the asymmetry of the coupling for the appearance of the Kondo peak at nonzero voltages and qualitatively explain recent experiments.

PACS numbers: 73.23.-b, 73.63.Kv

## I. INTRODUCTION

Recent advances in nanotechnology have allowed the fabrication of structures containing quantum dots coupled to the external environment. The quantum dot consists of finite number of electrons confined to the small region of space. It behaves like an impurity in a metal [1] and allows the study of the many body correlations between electrons. However, unlike an impurity which parameters are fixed, the coupling of the quantum dot to the external leads and its other parameters can be changed in a highly controlled way. Most importantly the non-equilibrium transport [2] can also be studied.

The discovery [3, 4] of the Kondo effect [5] in the quantum dots connected to external leads by tunnel junctions has resulted in an increased experimental [6]–[13] and theoretical [15]–[20] interest in this many body phenomenon. The Kondo effect in the quantum dot manifests itself at temperatures  $T$  lower than the Kondo temperature  $T_K$  as an increased conductance  $G$  through the system. It is due to the formation of the so called Abrikosov-Suhl or Kondo resonance at the Fermi energy. This is a many body singlet state involving spin on the the quantum dot and the electrons in external leads.

The experiments [3, 4, 6, 8] have confirmed the validity of the theoretical picture. They also discovered phenomena the explanation of which requires new theoretical ideas. In particular they have shown the non-orthodox and unexpected behavior of the systems in the Kondo regime. These are inter alia the observation of the Kondo peak at nonzero source-drain voltage [11, 12], absence of the odd-even parity effects expected for these systems [13] and observation of the singlet-triplet transition in a magnetic field. Besides the non-linear current-voltage characteristics it has been possible to measure charge distribution which led to the conclusion of spin-charge separation in a Kondo regime, observe the evolution of the transmission phase [9] and the detection of two different energy scales [10] related to two stages of the spin screening process in systems with spin  $S = 1$ , with one of the Kondo temperatures as high as 4K.

The great progress in theoretical understanding of the Kondo physics in real quantum dots has been made dur-

ing last decade. The theory has concentrated on such important aspects as the Kondo-driven transport in multilevel quantum dots [15], the coupled quantum dots [14], double-dot structures in which existence of the Kondo effect without spin-degree of freedom and new singlet-triplet effects have been predicted [18], the nature (weak vs strong coupling) of the Kondo effect at high voltage [19], the spin-charge separation in the strongly correlated quantum dot [17], the systems driven out of equilibrium by different means [20] etc..

Here we shall focus our attention on the experimental observation [11, 12] of the Kondo effect at nonzero source drain voltages. To state the problem in the right perspective let us remind that in systems containing quantum dot, the Kondo effect manifests itself at low temperatures as an enhanced conductance observed at zero source-drain voltage,  $V_{SD} = 0$  [1, 2, 5]. Occasionally, the Kondo peak in conductance appearing at nonzero voltages  $V_{SD} \neq 0$  [11] has been observed and this unusual behavior, called anomalous Kondo effect remains unexplained. Recently this phenomenon has been studied systematically [12]. The authors have fabricated the dot coupled weakly to one and strongly to another lead and observed the evolution of the peak at  $V_{SD} \neq 0$ . The source-drain voltage  $V_{SD}$ , at which the peak appears, scales roughly linearly with a gate voltage,  $V_g$ . In the experimental setup [12] the additional electrode determines the asymmetry in the coupling of the dot to left and right leads.

It is the purpose of this paper to study the anomalous Kondo peak observed at non zero voltage. We shall present the results of the model calculations based on the non-equilibrium transport theory [21] applied to the quantum dot described by the Anderson model [22] with asymmetric coupling to the leads. As we shall see the asymmetry in the couplings is the main factor which leads to this anomalous Kondo effect. The experimentally observed shifts of the Kondo peak to higher values of  $V_{SD}$  with increasing gate voltage can be satisfactorily explained by assuming that the values of the left and right barriers change together with the gate voltage, while the asymmetry in the couplings remains constant. This scenario is realized in experiment [12].

The organization of the rest of the paper is as follows. In section II we introduce the model, give the formula for the current through the quantum dot and discuss briefly the methods (equation of motion (EOM) with slave boson representation of electron operators and non-crossing approximation (NCA)) used to calculate on-dot Green's function relegating some technical details to the appendix. In section III we present the results of our numerical calculations of the tunneling conductance across the asymmetrically coupled single level quantum dot in  $U = 1$  limit. Conclusions are given in section IV.

## II. THE THEORY

For the sake of simplicity we discuss here the dot with single energy level. The theoretical analysis of the transport through quantum dot usually starts with the following, Landauer type, formula [2] for the current

$$J = \frac{e}{\hbar} \sum_{\sigma} \frac{X_L(\sigma) X_R(\sigma)}{X_L(\sigma) + X_R(\sigma)} \frac{1}{2\pi} \text{Im} G^r(\sigma + i0^+) \quad (1)$$

Here  $f(\epsilon)$  denotes the Fermi distribution function for lead with chemical potential  $\mu$ ,  $G^r(\epsilon)$  is the (retarded) impurity Green's function and  $X_{\alpha}(\epsilon) = 2\pi \sum_k V_k^{\alpha} f_k(\epsilon - \epsilon_k)$  is the effective coupling of localized electron to conduction band.

The current  $J$  flowing across the system depends on the source-drain voltage  $V_{SD} = (\mu_L - \mu_R)/e$ , where  $e$  is the electron charge. The differential conductance of the system defined as  $G(V_{SD}) = \frac{dJ(V_{SD})}{dV_{SD}}$  is directly measured experimentally [3].

To calculate the on-dot Green's function  $G(\epsilon + i0^+)$  we shall describe the dot coupled to the external leads by the single impurity Anderson Hamiltonian [22]

$$H = \sum_k \epsilon_k c_k^{\dagger} c_k + E_d \sum_{\sigma} d_{\sigma}^{\dagger} d_{\sigma} + U n_{\uparrow} n_{\downarrow} + \sum_k (V_k c_k^{\dagger} d + H.c.) \quad (2)$$

Here  $\epsilon_k = \epsilon_k^R/L$  denote the right (R) or the left (L) lead in the system. Other symbols have the following meaning:  $c_k^{\dagger}$  ( $c_k$ ) denotes creation (annihilation) operator for a conduction electron with wave vector  $\mathbf{k}$ , spin  $\sigma$  in the lead,  $V_k$  is the hybridization matrix element between conduction electron of energy  $\epsilon_k$  in the lead and localized electron on the dot.  $E_d$  is the single particle energy at the dot.  $n_{\sigma} = d_{\sigma}^{\dagger} d_{\sigma}$  is the number operator for electrons with spin up localized on the dot and  $U$  is the (repulsive) interaction energy between two electrons. Our calculations are restricted to very low temperatures, much smaller than the orbital level spacing in quantum dot so it is legitimate to consider single energy level  $E_d$ .

There are various methods [2] of calculating the on-dot Green's function entering the current (1). Here we shall apply two of them: equation of motion method (EOM) and non-crossing approximation (NCA). In both cases we assume that the Coulomb repulsion  $U$  between electrons on the dot is the largest energy scale. Therefore we take the limit  $U \rightarrow \infty$ . The original correlated electron operators are expressed as products of auxiliary fermion and boson ones [2].

When using equation of motion method (EOM) we apply a mean field like approximation for the slave bosons and calculate all matrix elements of the Keldysh Green's functions, including the distribution one [23]. In the process we consistently decouple all elements of the higher order Keldysh Green functions [24]. The relevant formulae and some technical details can be found in the appendix. As we shall see the method gives correct position of the Kondo peak. However, like the standard EOM it leads to incorrect width of the peak and the occupations. Therefore we have used the non-crossing approximation (NCA), which is generally accepted technique of solving the problem at hand [5]. In the NCA one maps the infinite  $U$  Anderson model onto the slave boson one and calculates both boson and fermion propagators. They are expressed by the coupled integral equations [2].

Where appropriate we shall present the results obtained by both techniques.

## III. NUMERICAL RESULTS

Let us first discuss the relation between the experimental parameters and those entering the model and the theory. The effective coupling  $X_L$  and  $X_R$  have been estimated in ref.[12] to be 170 eV and 80 eV respectively. Their values and the ratio  $X_L/X_R = 2$  have been argued to remain constant during the measurements. The source-drain voltage  $V_{SD}$  is the difference of the chemical potentials of the external leads. The (back)gate voltage  $V_g$  controls the position of the on-dot energy level  $E_d$ . As already mentioned we stick here to the  $U = 1$  limit. In this limit there can be at most a single electron with energy  $E_d$  on the dot at a time.

We start the presentation of the results with the comparison of the (equilibrium) density of states of a quantum dot coupled to two leads obtained by means of NCA and EOM approaches. It is shown in the Fig. (1). The main features of the DOS remain the same in both approaches. However the height and the width of the Kondo peak is much larger in the NCA. Moreover the spectral weight is shifted towards higher energies. In turn this leads to different occupations shown in the inset of the Fig.(1).

Now let's turn to the nonequilibrium ( $\mu_L \neq \mu_R$ ) density of states. In this case the high energy features to large extent remain the same as in equilibrium (see Fig.(1)), so the only low energy DOS is shown in the Fig.(2). The upper panel presents results obtained

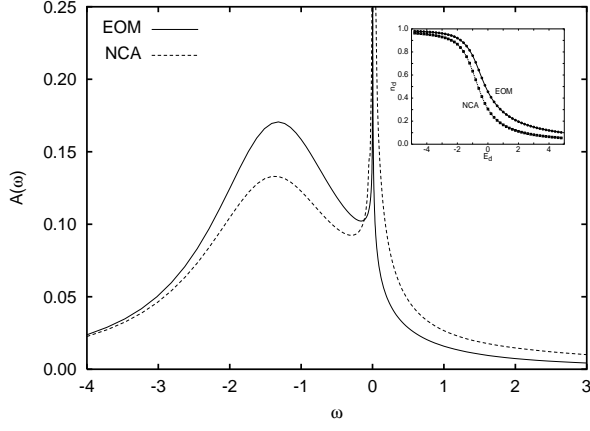


FIG. 1: The equilibrium density of states on the quantum dot obtained within EOM (solid line) and NCA (dashed line). Note the relative shift of the spectral weight with respect to the chemical potential  $\mu = 0$  which results in different occupations shown in the inset. The parameters are:  $E_d = 2$ ,  $\Gamma_L = \Gamma_R = 1$  and  $T = 10^{-3}$ .

via equation of motion technique for Keldysh (matrix) Green's function. In the lower panel the results obtained with the non-crossing approximation are shown. The coupling is asymmetric with  $\Gamma_L = \Gamma_R = 2$  (dashed lines) and  $\frac{1}{2}$  (dotted lines). The case of the symmetric coupling  $\Gamma_L = \Gamma_R$  is also shown (solid lines) for comparison. Few features have to be noted. First we see that the Kondo peak is always located at energies coinciding with those of the Fermi levels of the leads. Thus in non-equilibrium we get (in the density of states) two Kondo resonances pinned to Fermi energies of the left and right electrodes. Note also that the heights of the respective Kondo resonances strongly depend on the value of the hybridization. The overall shape of the density of states is similar. The positions of the Kondo peaks are roughly the same but they differ in width and heights. The peaks obtained in EOM, are much narrower and smaller. As a result the curves in figure (2a) differ from that in figure (2b).

These details in the energy dependence of the density of states may shortly be a matter of direct measurements. In fact it has been recently predicted theoretically [25] that the on-dot density of states can be measured in a device containing quantum dot coupled to three leads. The very weakly coupled third lead will act as a tunneling tip in conventional tunneling microscope and will probe the non-equilibrium density of states. The conductance spectrum measured by this additional electrode has been shown [25] to follow the non equilibrium density of states, like one shown in Fig.(2).

Returning to our main subject we show in Fig.(3) the differential conductance spectrum corresponding to the same 'experimental setup' as discussed previously in connection with figure (2). For comparison we have also plotted in this figure the conductance through the symmetrically coupled quantum dot. In the symmetric situation

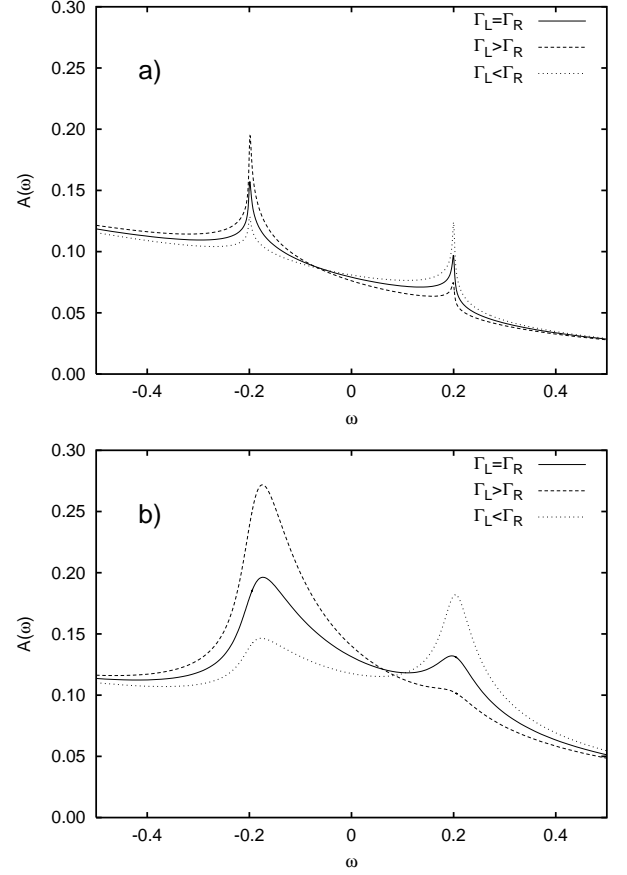


FIG. 2: The nonequilibrium density of states obtained within a) -EOM and b) -NCA for the symmetric  $\Gamma_L = \Gamma_R$  (solid lines) and asymmetrically coupled quantum dot with  $\Gamma_L = 2\Gamma_R$  (dashed) and  $\Gamma_L = \frac{1}{2}\Gamma_R$  (dotted lines).  $\Gamma_R = \Gamma_L = 0.2$  and the other parameters are the same as in Fig. (1).

( $\Gamma_L = \Gamma_R$ ) the Kondo resonance is located exactly at zero bias ( $V_{DS} = 0$ ), but for  $\Gamma_L > \Gamma_R$  ( $\Gamma_L < \Gamma_R$ ) it is shifted to the negative (positive) voltages  $V_{DS}$ . This finding is in nice qualitative agreement with the experimental studies on the transport through the quantum dot in the presence of the asymmetric barriers [12]. While the observed shifts calculated within EOM and NCA are of comparable magnitude the clear differences in their shape are visible. The NCA peaks are much higher and more symmetric in vicinity of their maxima. For asymmetric coupling the Kondo resonance in the conductance is pinned to the position of the Fermi level of that lead which is more strongly coupled (larger  $\Gamma$ ) to the dot. It is thus mainly the relative coupling which rules the value of the shift.

In Fig.(4) we show the systematic change of the  $G(V_{DS})$  with increasing asymmetry  $\Gamma_L = \Gamma_R$  of the coupling. The upper curves in both panels corresponds to  $\Gamma_L = \Gamma_R = 5.5$  while lower one is for symmetric coupling  $\Gamma_L = \Gamma_R = 1$  in steps of 0.5. The increase of the asymmetry  $\Gamma_L = \Gamma_R$  from 1 to 5.5 continuously moves the Kondo peak away from  $V_{SD} = 0$  position. We have checked

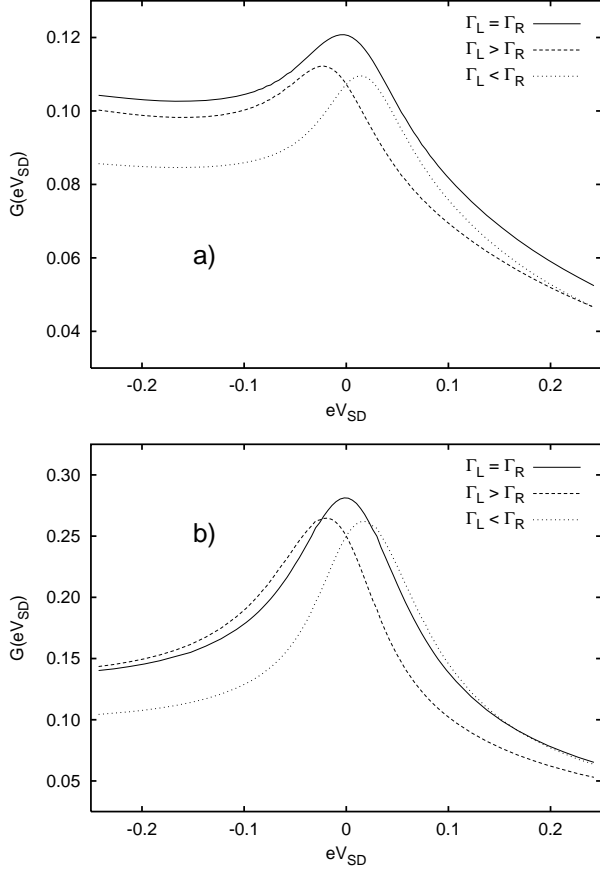


FIG. 3: The differential conductance ( $G(eV_{SD}) = dJ/d(eV_{SD})$ ) obtained within a) - EOM and b) - NCA for the symmetric  $\Gamma_L = \Gamma_R$  (solid lines) and asymmetrically coupled quantum dot with  $\Gamma_L = 2\Gamma_R$  (dashed) and  $\Gamma_L = \frac{1}{2}\Gamma_R$  (dotted lines).

that increasing asymmetry to still higher values does not lead to bigger shifts. This is easy to understand as for large asymmetry one of barriers is not transparent enough to produce the clear Kondo resonance in the density of states.

The position of the on-dot electron energy level  $E_d$  influences anomalous Kondo peak for the asymmetric dot with  $\Gamma_L = \Gamma_R = 2$  to lesser extent. It is only important that it takes a value appropriate for observing a Kondo resonance. For all appropriate  $E_d$  the shifts are of comparable magnitudes.

The data displayed in the figure (4) qualitatively agree with those plotted in figure (5) of [11] and figure (3) of [12]. However, theoretical shifts of the Kondo peak position are smaller than the experimental.

There may be additional factors which affect the position of the peaks. We have checked that the energy dependence of  $\Gamma_{L,R}$  introduces only small quantitative differences in the density of states and differential conductance, and does not lead to better agreement between theory and experiment. Similarly the calculations within EOM approach for finite values of  $U$  show that finite

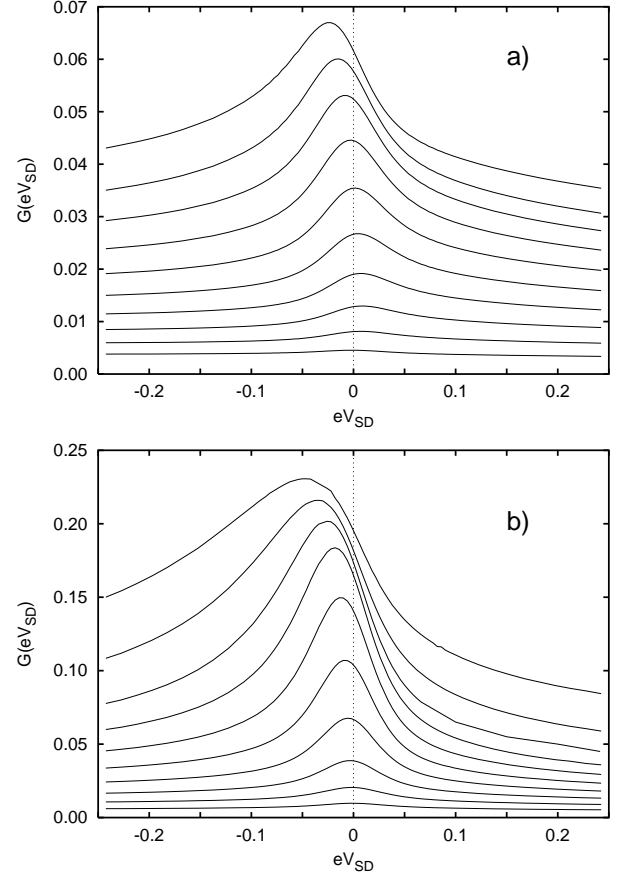


FIG. 4: The differential conductance obtained within a) - EOM and b) - NCA for the different asymmetric couplings. The lower curve is for  $\Gamma_L = \Gamma_R$  while the upper one -  $\Gamma_L = 5.5\Gamma_R$ . Other parameters are  $E_d = 10$  and  $T = 10^{-2}$  in units of  $\Gamma_R$ .

$U$  leads to minor corrections as also does the presence of the additional energy levels in the vicinity of Fermi energy. In all the cases studied one gets usual behavior with Kondo peak located at  $V_{SD} = 0$  for symmetric coupling to both leads and the anomalous Kondo effect for asymmetric coupling. This proves the importance of the asymmetry in the observation of it.

In experimental setup [12] the changes of the gate voltage  $V_g$ , which in first place affect the position of the electron energy level also modify the height of the barriers and their transparency  $V_k$ . This effect is of special importance in the quantum dots doped in the two dimensional electron gas where the voltage at a single electrode couples capacitively to other electrodes [26]. If we assume that (as in experiments)  $\Gamma_L = \Gamma_R$  remains constant ( $= 2$ ) and that the decrease of the energy  $E_d$  is accompanied by the simultaneous increase of the couplings  $\Gamma_R$  and  $\Gamma_L$  then the calculated shifts get larger.

The occurrence of the Kondo resonance is possible at low enough temperature. It is also well known [2] that changes of temperature move slightly the Kondo peak. We have checked this and found that if temperature is

raised the position of the peak moves slightly away from the  $V_{SD} = 0$ . At finite temperature the occupation of the dot changes and the Abrikosov-Suhl resonances smear out and this leads to small changes in the position of the Kondo peak.

We thus have combined all above contributions, i.e. asymmetry in the couplings  $\Gamma_L \neq \Gamma_R$ , their  $E_d$ -dependence, and assumed high enough, but still below  $T_K$ , temperature to get larger shifts of the Kondo peak. We have

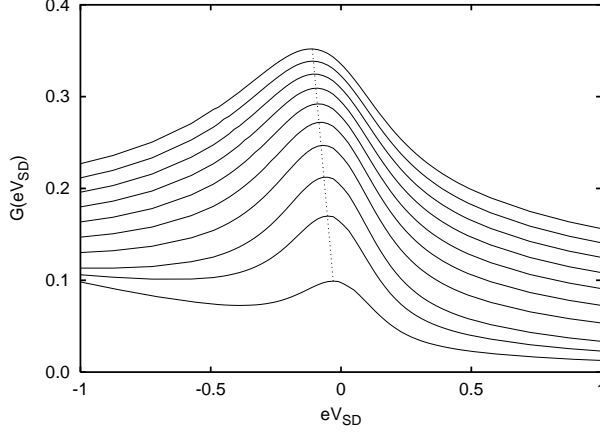


FIG. 5: The NCA calculated differential conductance as a function of source-drain voltage  $V_{SD}$  for various values of the  $E_d$  and  $\Gamma_L, \Gamma_R$  at fixed  $\Gamma_L = \Gamma_R = 2$ . The lowest curve correspond to  $E_d = 3$ ,  $\Gamma_L = 1$ , while upper one is for  $E_d = 12$ ,  $\Gamma_L = 6.4$  in units of  $\Gamma_0$  equal to initial coupling of the left lead. The temperature  $T = 5 \cdot 10^{-2}$  is below estimated Kondo temperatures.

shown the results in Fig.(5). The various curves have been calculated for  $T = 5 \cdot 10^{-3}$  which is below Kondo temperature. In the figure the change of the position of the on dot energy level is accompanied by the simultaneous change of the barrier transparency. The bottom curve in figure (5) corresponds to  $E_d = 3 \Gamma_0$ ,  $\Gamma_0 = \Gamma_L$ , while the upper one corresponds to  $E_d = 12 \Gamma_0$ ,  $\Gamma_L = 6.4 \Gamma_0$ . Here  $\Gamma_0$  is equal to experimentally estimated value of the smaller of couplings [12]. The ratio  $\Gamma_R = \Gamma_L$  is kept constant and equal 2 as estimated in [12]. The data are in nice qualitative agreement with experiments. The theoretical shifts, however, are smaller than experimental by a factor of 5-10. To check whether this is due to different asymmetry ratio we plot in figure (6) the results obtained for  $\Gamma_R = \Gamma_L = 4$ . The shifts have increased.

#### IV. CONCLUSIONS

We have found that the emergence of the Kondo peak at non zero voltages  $V_{DS} \neq 0$  is caused by asymmetric coupling of the dot to the external electrodes. These results are in qualitative agreement with experimental data on the transport through the quantum dot asymmetrically coupled to the leads [11, 12]. The theoretical Kondo

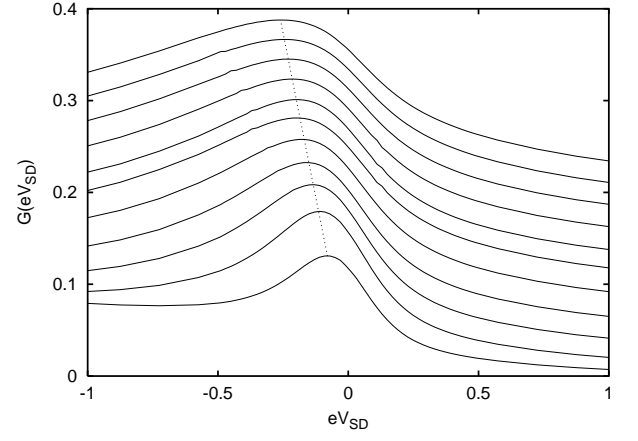


FIG. 6: The same as in Fig. (5) but for asymmetry  $\Gamma_L = \Gamma_R = 4$ . The lowest curve correspond to  $E_d = 4$ ,  $\Gamma_L = 1$ , while upper one is for  $E_d = 17.5$ ,  $\Gamma_L = 12.8$  in units of  $\Gamma_0$  equal to initial coupling of the left lead.

peaks in differential conductance, however, are narrower than experimental ones. Their maximum move to nonzero  $V_{SD}$  with increasing the asymmetry or the position of the on-dot energy level. The simultaneous change of  $E_d$  and  $\Gamma_L, \Gamma_R$  can semi-quantitatively explain experimental data. More experimental results are needed to draw firm conclusions such as the applicability of simple Anderson model to asymmetrically coupled quantum dots. It follows from the presented studies that the asymmetry of the couplings is a necessary ingredient for the explanation of the anomalous Kondo effect. Within the Anderson model one always gets normal Kondo effect for symmetric couplings and small shifts of the Kondo peak to non-zero voltages for asymmetric couplings. Our inability to explain quantitatively the experimental data may indicate the necessity of much better theoretical treatment of the model or even better model for the description of these complicated systems. There is a possibility that the experimentally observed features, even though similar to, do not represent genuine Kondo effect. In fact some researchers [27] have seen very small shifts, consistent with present calculations, even for quite asymmetrically coupled quantum dots.

#### Acknowledgments

This work has been partially supported by the State Committee for Scientific Research under grant 2P 03B 106 18. We thank unknown Referee for her/his comments on the first version of the paper.

#### APPENDIX A

To find the current across the system, Eq.(1), it is enough to calculate the on-dot retarded Green's function.

The NCA method to get  $G^r(i)$  has been extensively discussed previously [2] and there is no need to repeat its derivation again. For the sake of completeness let us only note that we have adapted the formulae derived in the second paper of the reference [2].

The EOM method to calculate the GF is straightforward and in  $U \rightarrow 1$  limit leads to

$$G^r(i) = \frac{1}{i - E_d} \frac{\text{Im } i}{\text{Im } i} \quad (\text{A } 1)$$

with the self-energy

$$\Sigma^r(i) = \sum_k \mathcal{J}_k^2 \frac{1 + f(i)}{i - \epsilon_k} \quad (\text{A } 2)$$

In the equation (A 1),  $\text{Im } i$  denotes the average on-dot occupation number of the spin electrons. In the equilibrium one calculates  $\text{Im } i$  self-consistently from

the retarded Green's function  $G^r(i)$ . Here we are dealing with nonequilibrium situation and  $\text{Im } i$  cannot be calculated directly from  $G^r(i)$ . Instead the nonequilibrium [21] Green's function technique has to be used. The occupation of the dot at time  $t$  is expressed via Keldysh "lesser" Green's function  $\text{Im } i = \langle c^\dagger(t) c(t) \rangle = -i G^<(t; t)$ . In the steady state one gets

$$\text{Im } i = -i \int_1^Z \frac{d!}{2} G^<(i) \quad (\text{A } 3)$$

This shows that the consistent calculations of the retarded GF requires the knowledge of "lesser" one. The equation of motion for the "lesser" GF has been formulated by Niu et al [23]. For the Hamiltonian of the form  $H = H_0 + H_I$  they derived the following general equation for the "lesser" GF

$$i\hbar \frac{d}{dt} \langle c_i^\dagger c_j^\dagger \rangle = g^<(i) \langle c_i^\dagger c_j \rangle + g^r(i) \langle c_i^\dagger c_j^\dagger \rangle + g^<(i) \langle c_i^\dagger c_j^\dagger \rangle + g^<(i) \langle c_i^\dagger c_j^\dagger \rangle \quad (\text{A } 4)$$

here  $g^{<(r)}(i)$  is the "lesser" (retarded) GF of the noninteracting part  $H_0$  of Hamiltonian.

To treat strong correlations we use the version [24] of

the slave boson technique and rewrite the Hamiltonian in the form

$$H^{SB} = \sum_k (\epsilon_k - \epsilon_d) c_k^\dagger c_k + \epsilon_d \sum_k f_k^\dagger f_k + \sum_k V_k (c_k^\dagger b_k^\dagger f_k + f_k^\dagger b_k c_k) \quad (\text{A } 5)$$

where new fermionic ( $f^\dagger; f$ ) and bosonic ( $b^\dagger; b$ ) operators have been introduced. Calculating the on-dot Green's function  $G^<(i) = \langle c_i^\dagger c_i^\dagger \rangle$  we have taken the third term of  $H^{SB}$  as an interaction part  $H_I$  and the rest two terms of it as  $H_0$ .

The average occupation number is found to be

$$\text{Im } i = \frac{1}{2} \sum_k \int_1^Z \frac{d!}{2} \text{Im } \Sigma^r(i) f(i) \mathcal{J}_k^2 \quad (\text{A } 6)$$

Note that in turn it depends on the retarded Green's function. This closes the system of equations.

- [1] T.K.Ng and P.A.Lee, Phys.Rev. 61, 1768 (1989); L.I.Glazman, and M.E.Raikh, Pis'ma Zh. Eksp. Teor. Fiz. 48, 378 (1988) [Engl. transl. JETP Lett. 47, 452 (1988)]; S.Herscheid, J.H.Davies, and J.W.Wilkins, Phys. Rev. Lett. 67, 3720 (1991); Phys. Rev. B 46, 7046 (1992).
- [2] Y.Meir N.S.Wingreen, and P.A.Lee, Phys.Rev.Lett. 70, 2601 (1993); N.S.Wingreen, and Y.Meir, Phys.

- Rev. B 49, 11040 (1994); Y.Meir, N.S.Wingreen, P.A.Lee, Phys.Rev.Lett. 66, 3048 (1991).
- [3] D.Goldhaber-Gordon, H.Shtrikman, D.Mahalu, D.Abusch-Magder, U.Meirav, M.A.Kastner, Nature 391, 1569 (1998).
- [4] S.M.Cronenwett, S.M.Maurer, S.R.Pate, C.M.Marens, C.I.Dumoz, J.S.Harris, Jr., Phys.Rev.Lett. 81, 5904 (1998); S.M.Cronenwett, T.H.Oosterkamp,

- and L. P. Kouwenhoven, *Science* 281, 540 (1998).
- [5] A. C. Hewson *The Kondo Problem to Heavy Fermions* (Cambridge University Press, Cambridge, UK, 1993); L. Kouwenhoven, L. Glazman, *Phys. World*, January 2001, p. 33.
- [6] D. Goldhaber-Gordon, J. Gores, M. A. Kastner, H. Shtrikman, D. Mahalu, and U. Meirav, *Phys. Rev. Lett.* 81, 5225 (1998).
- [7] S. Sasaki, S. De Franceschi, J. M. Elzerman, W. G. van der Wiel, M. Eto, S. Tarucha, L. P. Kouwenhoven, *Nature* 405, 764 (2000).
- [8] W. G. van der Wiel, S. De Franceschi, T. Fujisawa, J. M. Elzerman, S. Tarucha, L. P. Kouwenhoven, *Science* 289, 2105 (2000).
- [9] Y. Ji, M. Heiblum, D. Sprinzak, D. Mahalu, H. Shtrikman, *Science* 290, 779 (2000); Y. Ji, M. Heiblum, H. Shtrikman, *Phys. Rev. Lett.* 88, 076601 (2002).
- [10] W. G. van der Wiel, S. De Franceschi, J. M. Elzerman, S. Tarucha, L. P. Kouwenhoven, J. Motohisa, F. Nakajima, T. Fukui, *Phys. Rev. Lett.* 88, 126803 (2002).
- [11] J. Schmid, J. Weis, K. Eberl, K. von Klitzing, *Physica B* 256-258, 182 (1998).
- [12] F. Simmel, R. H. Blick, J. P. Kotthaus, W. Wegscheider, M. Bichler, *Phys. Rev. Lett.* 83, 804 (1999).
- [13] J. Schmid, J. Weis, K. Eberl, K. v. Klitzing, *Phys. Rev. Lett.* 84 5824 (2000).
- [14] T. Ivanov, *Europhys. Lett.* 40, 183 (1997); T. Ivanov, *Phys. Rev. B* 56, 12339 (1997); T. Aono, M. Eto, K. Kawamura, *J. Phys. Soc. Jpn.* 67, 1860 (1998); R. Aguado, D. C. Langreth, *Phys. Rev. Lett.* 85, 1946 (2000).
- [15] T. Inoshita, A. Shimizu, Y. Kuramoto, H. Sakaki, *Phys. Rev. B* 48, 14725 (1993); T. Inoshita, Y. Kuramoto, H. Sakaki, *Superlatt. and Microstr.* 22, 75 (1997); T. Pohjola, J. König, M. M. Salomaa, J. Schmid, H. Schoeller, G. Schon, *Europhys. Lett.* 40, 189 (1997); A. L. Chudnovsky, S. E. Ulloa, *Phys. Rev. B* 63, 165316 (2001); M. Pustilnik, L. I. Glazman, *Phys. Rev. Lett.* 87, 216601 (2001).
- [16] M. Pustilnik, Y. Avishai, K. Kikoin, *Phys. Rev. Lett.* 84, 1756 (2000); M. Pustilnik, L. I. Glazman, *Phys. Rev. Lett.* 85, 2993 (2000); M. Pustilnik, L. I. Glazman, *Phys. Rev. B* 64, 045328 (2001); M. Eto, Y. V. Nazarov, *Phys. Rev. Lett.* 85, 1306 (2000); M. Eto, Y. V. Nazarov, *Phys. Rev. B* 64, 085322 (2001); D. Giuliano, A. Tagliacozzo, *Phys. Rev. Lett.* 84, 4677 (2000); D. Giuliano, B. Jouault, A. Tagliacozzo, *Phys. Rev. B* 63, 125318 (2001); W. Hofstetter, H. Schoeller, *Phys. Rev. Lett.* 88, 016803 (2002).
- [17] L. I. Glazman, F. W. J. Hekking, A. I. Larkin, *Phys. Rev. Lett.* 83, 1830 (1999); A. Silva, S. Levit, *cond-mat/0107595*
- [18] Q. Sun, H. Guo, *cond-mat/0109145*; T. Aono, M. Eto, *Phys. Rev. B* 64, 073307 (2001); V. N. Golovach, D. Loss, *cond-mat/0109155*.
- [19] A. Kaminski, Y. V. Nazarov, L. I. Glazman, *Phys. Rev. B* 62, 8154 (2000); P. Coleman, C. Hooley, O. Parcollet, *Phys. Rev. Lett.* 86, 4088 (2001); A. Rosch, J. Kroha, P. Woelke, *Phys. Rev. Lett.* 87, 156802 (2001); Y. W. Lee, Y. L. Lee, *cond-mat/0105009*.
- [20] M. H. Hettler, H. Schoeller, *Phys. Rev. Lett.* 74, 4907 (1995); T. K. Ng, *Phys. Rev. Lett.* 76, 487 (1996); Y. Goldin, Y. Avishai, *Phys. Rev. Lett.* 81, 5394 (1998); A. Kaminski, Y. V. Nazarov, L. I. Glazman, *Phys. Rev. Lett.* 83, 384 (1999); P. Nordlander, N. S. Wingreen, Y. Meir, *Phys. Rev. B* 61, 2146 (2000); M. Plihal, D. C. Langreth, P. Nordlander, *Phys. Rev. B* 61, R13341 (2000); M. Plihal, D. C. Langreth, P. Nordlander, *cond-mat/0108525*; A. Schiller, S. Hershfeld, *Phys. Rev. B* 62, R16271 (2000); R. Lopez, R. Aguado, G. Platero, C. Tejedor, *Physica E* 6, 379 (2000); R. Lopez, R. Aguado, G. Platero, C. Tejedor, *Phys. Rev. B* 64, 075319 (2001); R. Aguado and D. C. Langreth, *Phys. Rev. Lett.* 85, 1946 (2000).
- [21] L. V. Keldysh, *Zh. Eksp. Teor. Fiz.* 47, 1515 (1965) [*Sov. Phys. JETP* 20, 1018 (1965)]; H. Haug, A. P. Jauho, "Quantum Kinetics in Transport and Optics of Semiconductors", Springer Verlag, Berlin 1996.
- [22] P. W. Anderson, *Phys. Rev.* 124, 41 (1961).
- [23] C. Niu, D. L. Lin, T. H. Lin, *J. Phys. Condens. Matter* 11, 1511 (1999).
- [24] M. Krawiec, K. I. Wysokinski, *Solid State Commun.* 115, 141 (2000).
- [25] Q. Sun, H. Guo, *Phys. Rev. B* 64, 153306 (2001); E. Lebanon, A. Schiller, *Phys. Rev. B* 65, 035308 (2002).
- [26] T. Christen and M. Buttiker, *Europhys. Lett.* 35, 523 (1996); C. A. Staord, *Phys. Rev. Lett.* 77, 2770 (1996).
- [27] D. Goldhaber-Gordon, private communication.